Computer Vision for Human Stem Cell Derived Cardiomyocyte Classification: the Induced Pluripotent vs Embryonic Stem Cell Case Study

M Paci[1], L Nanni[2], A Lahti[3], S Severi[1], K Aalto-Setälä[3,4], J Hyttinen[5]

[1]DEIS, University of Bologna, Cesena, Italy
[2]DEI, University of Padua, Padua, Italy
[3]IBT, University of Tampere, Tampere, Finland
[4]Tampere University Hospital, Heart Center, Tampere, Finland
[5]BME, Tampere University of Technology, Tampere, Finland

Abstract

Human induced pluripotent stem cell-derived cardiomyocytes (hiPSC-CMs) represent a potential valuable alternative to human embryonic stem cell-derived cardiomyocytes (hESC-CMs) for the lack of ethical issues and their patient-specificity. Recent studies showed hiPSC-CMs behave like hESC-CMs in terms of membrane currents, contractility and frequency of spontaneous pacing but their similarities need to be studied more. In this work we applied a well tested image processing approach based on texture feature extraction (local binary patterns, Haralick features and threshold adjacency statistics) and classification by support vector machines to hiPSC-CMs and hESC-CMs images from contrast phase microscopy. Our results suggested a good discrimination power of the chosen feature set meaning that some structural differences may still remain between the two cell classes.

1. Introduction

Human induced pluripotent stem cells (hiPSCs) represent a promising tool for cell therapies such as autologous implantation and for drug testing since genetic mutations affecting the patient are reflected by the differentiated hiPSCs. Experiments on hiPSC-derived cardiomyocytes (hiPSC-CMs) showed expression of the majority of ion channels identified in human embryonic stem cell-derived cardiomyocytes (hESC-CMs) [1]. Moreover, no significant differences in response to cardioactive drugs between hiPSC-CMs and hESC-CMs were reported in literature [1]. Anyway defining whether hESCs and hiPSCs are equivalent remains a pressing issue. Aim of our work is assessing if differences between hiPSC-CMs and hESC-CMs emerge from texture analysis of contrast phase microscopy images reflecting possible structural differences.

2. Methods

Computer vision techniques such as texture analysis and classification were intensely used for solving different problems, from face recognition [2] to fingerprint matching [3], but their potential is getting more and more important also in the biological field [4,5]. In this paper texture analysis and classification are used to discriminate between hESC-CMs (H7, WiCell Research Institute) and hiPSC-CMs (derived from a healthy individual, IBT, Tampere, Finland).

2.1. Dataset

Dataset includes 10000 images grabbed from 100 different movies (acquisition setup: microscope Nikon TS100F, camera Optika Digi-12) of beating cardiomyocytes, 17 derived from hESCs and 83 derived from hiPSCs. From each movie 100 frames were grabbed. Illustrative pictures for both classes are shown in Fig. 1.

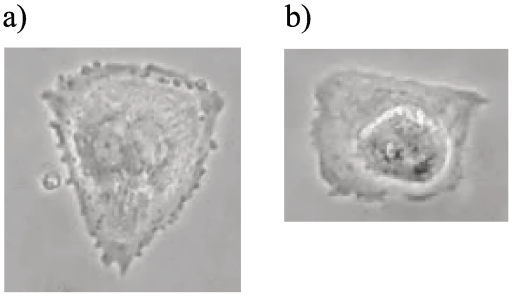

Figure 1. Representative pictures for hESC-CMs (a) and hiPSC-CMs (b).

2.2. Texture features

To avoid the overfitting problem, we chose a well-assessed texture feature set from literature [4]: uniform

rotation invariant local binary patterns (LBP) [6], Haralick statistics (HAR) [7] and threshold adjacency statistics (TAS) [8]. LBP represents one of the best assessed operators in texture analysis during this decade in particular for its invariance against any monotonic transformation of the grey scale. In its basic formulation, the $LBP_{P,R}$ operator is calculated for every pixel of a picture considering the joint distribution of the grey intensity levels in a circular local neighbourhood of radius R and P pixels (g_i) with respect to the grey level of the central pixel (g_c). A binary pattern is so calculate considering the sign of the difference between g_i and g_c in the circularly symmetric neighbourhood, according to Eq. 1 and Eq. 2:

$$s(x) = \begin{cases} 1, x \geq 0 \\ 0, x < 0 \end{cases} \quad (1)$$

$$LBP_{P,R} = \sum_{p=0}^{P-1} s(g_p - g_i) 2^p \quad (2)$$

LBP patterns are summarized in a N bins histogram in which each bin represents the occurrence number of a pattern in the picture: since we used the rotation invariant uniform LBP formulation, N = P+2, thus reducing the number of pattern calculated in the picture. The configurations {P, R, N} proposed in the original paper [6] were tested: {8, 1, 10}, {16, 2, 18} and {24, 3, 26} (Fig. 2). HAR statistics are calculated from the gray level co-occurrence matrix G in Eq. 3

$$G = \begin{bmatrix} p(1,1) & p(1,2) & \dots & p(1,N_g) \\ p(2,1) & p(2,2) & \dots & p(2,N_g) \\ \vdots & \vdots & \ddots & \vdots \\ p(N_g,1) & p(N_g,2) & \dots & p(N_g,N_g) \end{bmatrix} \quad (3)$$

where N_g represents the number of grey levels and p(i,j) the probability a pixel of value i is contiguous to a pixel of value j. In this paper, the adjacency direction for the matrix G construction is 0° (horizontal). TAS statstics are calculated on the threshold images in the ranges (μ-30, μ+30), (μ-30, 255) and (μ, 255), μ average intensity, considering for each white pixel the number of white pixels surrounding it (0, 8) and normalizing them by the total number of white pixels in the threshold image. The final feature vector is thus composed by 54 LBP, 13 HAR and 27 TAS features for a total of 94 features extracted for each of the 10000 images.

2.3. Classification

Two different classifiers were tested in this work, a stand-alone Support Vector Machine (SVM) and a Random Subspace of SVM (RSSVM), as shown in Fig. 3. The Random Subspace method consists in training an ensemble of N_c classifiers using for each of them a subset of the original feature set. Considering a training set T containing Q features, each classifiers is trained using a subset T_i of T represented by Q·k features (0< k <1) randomly chosen among the Q original features. The purpose of using the Random Subspace is handling the problem of the correlation among the extracted features. In this work Q = 94, k = 0.5 and N_c = 52.

2.4. Protocols

Two different approaches were tested to assess he goodness of the chosen operators. The first protocol (P1) is the movie leave one out: 100 classification tests were performed considering as training set 99 cells (9900 pictures) and as test set 1 cell only (100 pictures). The purpose of these tests consists in assessing the successful classification of the test cell as hESC-CM or hiPSC-CM. Performances of this protocol were measured in term of Area Under ROC Curve (AUC, 0≤AUC≤1, 0=bad, 0.5=worthless, 1= perfect classification), both for frame classification and movie classification (average of the (RS)SVM decision values was used). The second protocol (P2) is a classic training/testing of the chosen classifier. As training set 17 hESC-CM and 21 hiPSC-CM movie were used (3800 pictures) while the remaining 62 hiPSC-CM cells (6200 pictures) were used as test set. Since AUC can not be used as a performance index (test set contains just 1 class), the probability of good classification was considered.

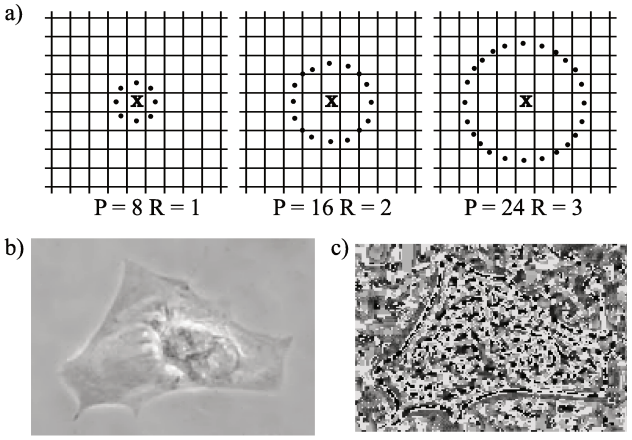

Figure 2. Local binary patterns: neighbor sets for different P and R (a). Representative picture before (b) and after (c) the application of the LBP operator.

3. Results

3.1. Protocol P1

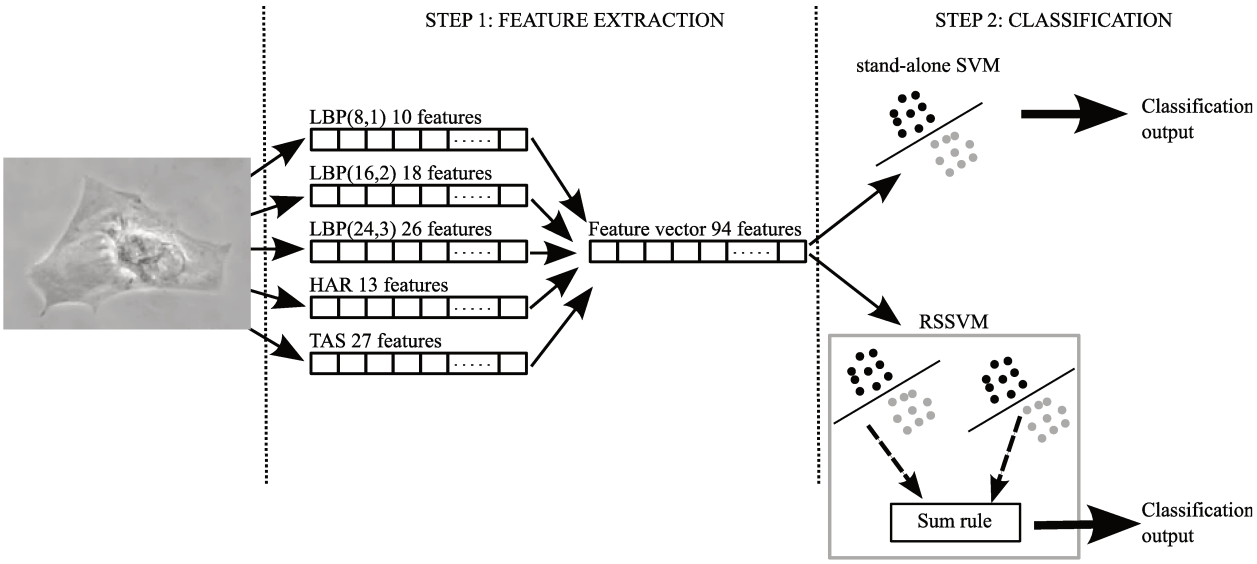

Figure 3. A complete schema of the proposed approach. Step 1 consists in feature extraction using $LBP_{8,1}$, $LBP_{16,2}$, $LBP_{24,3}$, HAR and TAS and concatenating all the feature in the total feature vector. In Step 2 classification is performed both by a stand-alone SVM and by a RSSVM

Results of the movie leave one out protocol are reported in Table 1. The best classification results for images and movies are reached using RSSVM.

Table 1. Movie leave one out (protocol P1) results. AUC is reported for stand-alone SVM and RSSVM both for image and movie classification.

	Image classification	Movie Classification
SVM	0.9376	0.9426
RSSVM	**0.9429**	**0.9468**

Table 2. Protocol P2 results. Number of correctly classified images and movies and accuracy (%) of classification.

	Image classification	ACC (%)	Movie Classification	ACC (%)
SVM	**4387**	**70.76**	43	69.35
RSSVM	4324	69.74	**44**	**70.97**

3.2. Protocol P2

Results of protocol P2 are reported in Table 2 in terms of correctly classified images and movies and accuracy of classification with respect to the 6200 pictures in the test set. As threshold to assign a picture/movie to one or to the other class, a probability (Pr) of 0.5 was chosen (Pr<0.5 means hESC-CM, Pr≥0.5 means hiPSC-CM). For movie classification the average of the picture probabilities was considered. These tests led to a good classification about in 70 % of cases.

4. Discussion and conclusions

In this paper we used a well-assessed combination of texture operators and classifiers [4] to show the opportunity to discriminate between hESC-CMs and hiPSC-CMs using images acquired with a not invasive technique (no staining, no dissociation or breaking up the cells). hiPSC-CMs are nowadays considered a more valuable opportunity than hESC-CMs in terms of regenerative medicine and drug or toxicant testing, in particular for the lack of ethical issues and for their patient-specificity. This last feature is particularly outstanding since cardiomyocytes differentiated from hiPSCs can reflect the same mutations found in the original patient [9,10]. The development of patient-specific cell lines carrying genetic mutations will open new challenges in development specific drugs for genetic cardiac disorders. A quite recent study [1] showed in hiPSC-CMs expression of genes coding for various ion channels responsible of membrane currents such as the sodium current I_{Na}, the L-type calcium current I_{CaL} and the HCN current I_f all involved in the spontaneous pacing of hiPSC-CMs. Moreover studying the response to cardioactive drugs (eg. adrenaline, isoprenalin and verapamil) in hESC-CMs and hiPSC-CMs no significant differences were found in rate of spontaneous beating and

contractility (calculated as the difference between diastolic and systolic major axes normalized by the diastolic major axis). Anyway a new study [11] found genomic modifications in iPSC induced from murine fibroblast and mammary cells according to two previously established protocols, suggesting that differences can still be present between iPSCs and ESCs. Our study supports the hypothesis that some structural differences may still remain between these two classes of cells, using non-invasive image processing/computer vision techniques and providing results in terms of AUC (>0.9) and good classification performances (~70%). More studies are still necessary to understand the possible biological explanation of our good classification results.

Acknowledgements

LBP Matlab implementation available at Outex site (http://www.outex.oulu.fi/).

HAR Matlab implementation available at http://read.pudn.com/downloads114/sourcecode/graph/479658/Haralick.m__.htm, (Haralick Texture Features Matlab Toolbox v0.1b, shalinig@ece.utexas.edu).

SVM implemented as in libsvm 2.9 (http://www.csie.ntu.edu.tw/~cjlin/libsvm/).

References

[1] Yokoo N, Baba S, Kaichi S, Niwa A, Mima T, Doi H, et al. The effects of cardioactive drugs on cardiomyocytes derived from human induced pluripotent stem cells. Biochemical and biophysical research communications. 2009;387(3):482-488.

[2] Ahonen T, Hadid A, Pietikäinen M. Face description with local binary patterns: application to face recognition. IEEE transactions on pattern analysis and machine intelligence. 2006;28(12):2037-2041.

[3] Nanni L, Lumini A. Local binary patterns for a hybrid fingerprint matcher. Pattern Recognition. 2008;41(11):3461-3466.

[4] Nanni L, Lumini A. A reliable method for cell phenotype image classification. Artificial intelligence in medicine. 2008;43(2):87-97.

[5] Vécsei A, Amann G, Hegenbart S, Liedlgruber M, Uhl A. Automated Marsh-like classification of celiac disease in children using local texture operators. Computers in Biology and Medicine. 2011;1-13.

[6] Ojala T, Pietikäinen M, Mäenpää T. Multiresolution Gray-Scale and Rotation Invariant Texture Classification with Local Binary Patterns. IEEE Transactions on Pattern Analysis and Machine Intelligence. 2002;24(7):971-987.

[7] Haralick R, Shanmugam K,, Dinstein I. Textural features for image classification. IEEE Transactions on Systems, Man, and Cybernetics. 1973;SMC-3610-3621.

[8] Hamilton N, Pantelic R, Hanson K, Teasdale R. Fast automated cell phenotype image classification. BMC bioinformatics. 2007;8(1):110.

[9] Yazawa M, Hsueh B, Jia X, Pasca AM, Bernstein JA, Hallmayer J, et al. Using induced pluripotent stem cells to investigate cardiac phenotypes in Timothy syndrome. Nature. 2011;471(7337):230-234.

[10] Matsa E, Rajamohan D, Dick E, Young L, Mellor I, Staniforth A, et al. Drug evaluation in cardiomyocytes derived from human induced pluripotent stem cells carrying a long QT syndrome type 2 mutation. European Heart Journal. 2011;32(8):952-962.

[11] Pasi CE, Dereli-Oz A, Negrini S, Friedli M, Fragola G, Lombardo A, et al. Genomic instability in induced stem cells. Cell Death and Differentiation. 2011;18(5):745-753

Address for correspondence.

Michelangelo Paci
Laboratorio di Ingegneria Biomedica
Università di Bologna
Via Venezia 52, 47521 Cesena (FC), Italy
michelangelo.paci@unibo.it